GCAGS JOURNAL
A Publication of the Gulf Coast Association of Geological Societies
www.gcags.org

CO_2 Sequestration Capacity Sectors in Miocene Strata of the Offshore Texas State Waters

David L. Carr, Kerstan J. Wallace, Changbing Yang, and Andrew J. Nicholson

Bureau of Economic Geology, Jackson School of Geosciences, University of Texas at Austin, University Station, Box X, Austin, Texas 78713–8924, U.S.A.

ABSTRACT

It was previously shown by the authors that the P_{50} static net CO_2 sequestration capacity estimated for Miocene strata beneath offshore Texas State Waters (OTSW) is 30.1 gigatonnes (Gt) of CO_2. The OTSW is the 16 km (10 mi) wide swath of Gulf of Mexico waters lying immediately seaward of the 590 km (367 mi) long Texas shoreline. This paper provides high-level decision-makers with further detail on CO_2 sequestration potential of the OTSW. We accomplished this by dividing the OTSW into seven sectors that are on the order of a Texas county in areal extent. For each sector we have calculated the CO_2 capacity, written a brief narrative pertaining to the geology and source-sink relationships, and created an informal (qualitative) rating as to the overall favorability (i.e., CO_2 sequestration potential) of the sector.

Our intent here is to provide broad guidance for understanding the distribution of the potential CO_2 capacity resource. Although there are many geologic details controlling the actual CO_2 capacity of a given reservoir, (e.g., fluid saturations, internal heterogeneity, top seal characteristics, and presence/degree of faulting), for our high-level result, the key factors controlling static CO_2 capacity estimates were the volume of net reservoir sandstone, the depth of reservoir occurrence, and the depth of geopressure.

The average area of each OTSW sector is 1395 km^2 (539 mi^2), and ranges from 815–1871 km^2 (315–722 mi^2). On average, sectors contain 4.3 Gt CO_2 (14% of Total OTSW) capacity, and range from 1.2–8.0 Gt CO_2. CO_2 capacity per unit area averages 3.0 megatonnes per square kilometer (Mt/km^2) or 7.8 megatonnes per square mile (Mt/mi^2) and varies geographically, ranging from 2.0–5.4 Mt/km^2 (5.1–14.1 Mt/mi^2).

Upper Texas coast sectors—Houston (8.0 Gt CO_2), Galveston (3.7 Gt CO_2), and Brazos (2.7 Gt CO_2)—together comprise almost half (47.8%) of the CO_2 capacity we estimated for the entire OTSW. These sectors have highly favorable carbon sequestration potential due to the presence of high net-to-gross (sandstone), relatively deep geopressure, and their occurrence in close proximity to a large number of CO_2 point sources. The Houston sector alone contains an estimated 80 yr of CO_2 storage of adjacent point-source emission at present rates. Central coast sectors—Matagorda, Corpus Christi, and South Padre—have moderate to good favorability. The Rio Grande sector of the southernmost Texas coast has the least favorable potential for CO_2 sequestration due to low sandstone content and shallow overpressure. If commercial-scale carbon sequestration operations commence in the United States, the OTSW appears to contain excellent sequestration targets.

INTRODUCTION

Geologic sequestration (GS) of carbon dioxide (CO_2) into saline formations has been proposed as a potentially viable method for reducing atmospheric greenhouse gas emissions and has been shown to be possible with existing technology (Gale et al., 2001; Holloway, 2001; Tsang et al., 2002; Bachu, 2003; Bachu and Gunter, 2003; Lackner, 2003; Eiken et al., 2011). Estimates of CO_2 storage potential have been generated for many sedimentary basins worldwide using a method that consists of a discounted pore-volume calculation. A recent median estimate of total CO_2 storage capacity for the United States is 2891 gigatonnes (Gt = 10^9 t) (DOE, 2015). Our recent estimate of total CO_2 storage capacity for the offshore Texas State Waters (OTSW) is 30.1 Gt of CO_2 (Carr et al., in press).

Texas leads the U.S. in CO_2 emissions, at 389 megatonnes (Mt = 10^6 t) of CO_2 (EPA, 2015). The proximity of many CO_2 point sources along the Texas coast highlights the potential advantage of CO_2 GS in subsurface reservoirs of the Texas coastal region (Fig. 1). In addition to this favorable source-sink relationship, the following properties together suggest that potentially high CO_2 storage volumes are present and an overall positive GS outlook exists for OTSW Miocene strata:

- The Gulf of Mexico Basin has been an active target for oil and gas production for more than 70 yr, and as a result, is densely populated with subsurface data.

Manuscript received March 22, 2016; revised manuscript received June 3, 2016; manuscript accepted June 17, 2016.

GCAGS Journal, v. 5 (2016), p. 130–140.

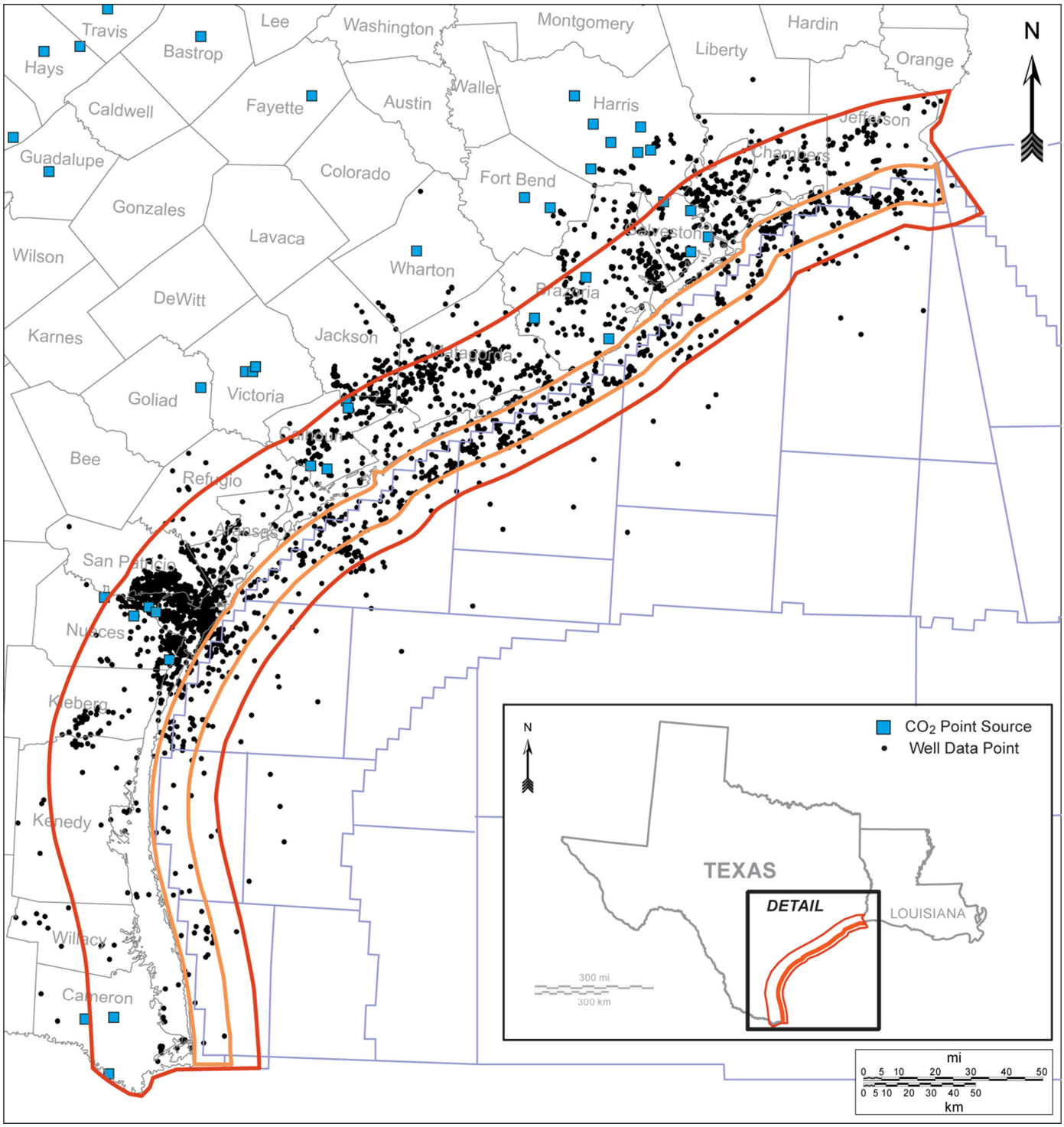

Figure 1. Location map showing study area and outline of the offshore Texas State Waters (orange polygon). Red polygon outlines the larger study area mapped by Carr et al. (in press). Blue squares represent major CO_2 point sources; note that those shown here represent a subset of the total point sources reported in Table 1. Black dots represent the 3184 wells for which wireline log data were available.

- Deep geological and operational knowledge exists in Texas.
- Numerous depleted oil and gas fields in the offshore Miocene may serve as initial storage or enhanced recovery targets.
- Sandstone reservoirs frequently exhibit both high porosity and permeability, averaging 28.2% and 338 md, respectively (Seni et al., 1997).
- Thick mudrock intervals that provide low-permeability regional seals are present, such as the *Amphistegina* B shale unit, with thickness up to 335 m (1100 ft) in the OTSW.
- Structural deformation from salt tectonism and extensional faulting has created numerous effective traps throughout the region.

- Much of the potential storage target in the Miocene interval occurs at favorable depths for storing CO_2 as a supercritical fluid (e.g., Elewaut et al., 1996) below approximately 915 m (3000 ft) to depths of approximately 3050 m (10,000 ft) or deeper, depending upon project economics.
- Environmental risks associated with sequestration are diminished given the lack of potable groundwater.
- Single leaseholder status (State of Texas) simplifies land rights and liabilities assessment.
- The region possesses cultural familiarity with offshore and subsurface operations.

Recent region-scale, quantitative capacity estimates for areas including the OTSW have been performed by Wallace et al. (2014) and Carr et al. (in press) support this contention. The results of these works suggest that if commercial-scale carbon sequestration operations commence in the United States, the OTSW would be an excellent target. The purpose of this paper is to provide decision-makers with a more localized perspective of the CO_2 sequestration potential for coastal Texas, such that it can be utilized as an early-phase, high-level screening tool. We have attempted to accomplish this by dividing the OTSW capacity estimate performed by Carr et al. (in press) into seven (7) geographically distinct sectors, from which we have calculated the static capacity and provided brief narratives pertaining to geological and source-sink specifics.

STUDY AREA, DATASET, AND METHODS

The focus of this study was the OTSW (orange polygon in Figure 1), which extends seaward for 16 km (10 mi) from the 591 km (367 mi) long Texas shoreline. The offshore Texas State Waters comprise 9875 km^2 (3813 mi^2) of the Gulf of Mexico inner shelf. The area of the OTSW is comparatively large, lying between the total areas for the states of Delaware (6446 km^2; [2489 mi^2]) and Connecticut (14,356 km^2 [5543 mi^2]) (U.S. Census Bureau, 2010a).

For making the capacity estimate, we used a Petra™ database containing 3184 wells for which wireline-log data were available that were located within, or adjacent to the OTSW (Fig. 1). Both raster logs and Log ASCII Standard (LAS) files were used to make stratigraphic interpretations and identify net sandstone reservoir intervals from which we subsequently made maps. Biostratigraphic reports (biostrat) were used to improve the accuracy of stratigraphic correlations. Biostrat reports are primarily composed of depth interpretations of key benthic foraminifera that are tied to geologic time zones within the Miocene and throughout the Cenozoic section in the Gulf of Mexico. The greatest concentrations of benthic microfossils are typically found in mudrock units that represent flooding/maximum flooding events. The reports are based on drill-cuttings data collected at 9 m (30 ft) intervals from the circulating mud system at the well site. As such, biostrat-report interpretations are subject to human error and dilution from mixing of cuttings from different depths and wellbore slough. We used biostrat picks as broad guidelines when correlating, rather than as "golden spike" ground truth.

We also integrated information from previous studies into the Petra™ electronic database, most notably works by Galloway and associates (e.g., Galloway, 2001) from the Gulf Basin Depositional Synthesis (GBDS) group at the University of Texas Institute for Geophysics, and Pitman's (2011; U.S. Geological Survey) GIS release of the Top of Overpressure map for the northern Gulf of Mexico Basin, which was modified from Wallace et al. (1981). Detailed methodology and workflows used to determine Miocene OTSW CO_2 storage capacity can be found in Wallace et al. (2014) and Carr et al. (in press). However, we present a brief overview to provide the reader with a contextual understanding of the process.

Methodology

CO_2 storage capacity in North America has been frequently performed by multiplying gross pore volume by CO_2 density with an efficiency factor (e.g., Vangkilde-Pedersen et al., 2009; Litynski et al., 2008). Goodman et al. (2011) proposed the following equation for determining CO_2 storage resource mass estimates (G_{CO_2}) in saline formations:

$$G_{CO_2} = A_t \, h_g \, \varphi_{tot} \, \rho \, E_{saline} \qquad \text{(Eq. 1)}$$

where A_t = total area, h_g = gross thickness, φ_{tot} = total porosity, ρ = CO_2 density, and E_{saline} = storage efficiency factor.

The storage efficiency factor (E) is determined at different probability values and for various lithologies through Monte Carlo simulation using field data from multiple oil and gas reservoirs in basins around the world. According to Goodman et al. (2011), the efficiency factor considers:

(1) net-to-total area—the fraction of the area that is suitable for CO_2 storage;
(2) net-to-gross thickness—the fraction of the interval with sufficient porosity and permeability to serve as an adequate CO_2 reservoir;
(3) effective-to-total porosity—the fraction of the pore space that is connected;
(4) volumetric displacement efficiency—the fraction of the reservoir volume accessible to CO_2 as a result of the density contrast between CO_2 and connate water; and
(5) microscopic displacement efficiency—the fraction of pore space that is occupied by immobile, residual fluids.

Using ranges of observed and hypothesized values for each of these parameters, Goodman et al. (2011) proposed a set of efficiency factors (E), ranging from 0.4 to 5.5%, for use in in sandstone, limestone, or dolomite saline aquifers and for probability values of P_{10}, P_{50}, or P_{90} that correspond to low, medium and high estimates, respectively (e.g., DOE, 2015). The regional capacity assessments provided by the DOE Regional Carbon Sequestration Partnerships are obtained using the methodology discussed above with assumed E values. These studies serve as the current primary basis for the estimate of total North American CO_2 storage capacity and, in turn, imply that there is potential for widespread carbon capture and storage development in the United States.

For the current study, we utilized the net reservoir sandstone refinement (equation 1) proposed by Wallace et al. (2014):

$$G_{CO_2net} = A_t \, h_{net} \, \varphi_{tot} \, \rho \, E_{net} \qquad \text{(Eq. 2)}$$

where G_{CO_2net} = net CO_2 saline aquifer capacity, h_{net} = net reservoir sandstone thickness, E_{net} = storage efficiency factor, adjusted for use of net reservoir sandstone thickness (rather than gross interval thickness), and remaining variables same as Equation 1.

Wallace et al. (2014) removed the net-to-gross considerations from the Goodman et al. (2011) equation (Equation 1 herein) and found that by using E_{net} = 4.5% (P_{50}), the results yield a more accurate capacity. Thus, by defining sandstone intervals in wireline well logs, uncertainty in the net-to-gross ratio consideration of the efficiency factor is significantly reduced, and one aspect affecting potential error in the regional assessment can be tested (Wallace et al., 2014). Following this methodology, we calculated capacity for each square kilometer (0.3861 mi^2) of the study area using gridded input maps generated from wireline well-log interpretations.

STRATIGRAPHY AND CAPACITY INTERVAL

Galloway et al. (2000) defined the top of the Miocene as a "flooding event associated with the *Robulus* E biostratigraphic top or, in parts of the basin where *Rob.* E is not picked, the slight-

ly older *Bigenerina* A marker" (Fig. 2). Offshore Texas biostratigraphic data (BOEM, 2010) contained about three times more *Bigenerina* A picks than *Robulus* E picks, so we opted to define the Miocene top using the *Bigenerina* A maximum flooding surface to facilitate consistency. Updip and landward (e.g., onshore), the top of the Miocene is much more difficult to define as the section thins and becomes dominated by more heterogeneous fluvio-deltaic facies.

The base of the Miocene is relatively easier to pick in the OTSW since it is marked by the Anahuac Shale (latest Oligocene). The *Discorbis gravelli* biostratigraphic zone approximately marks the Anahuac second-order maximum flooding and correlates to a strong warming event within the larger-scale cooling inferred to have taken place from the late Oligocene through early Miocene (Fillon et al., 1997; Fillon and Lawless, 2000). The Anahuac maximum flooding surface (MFS) provided a consistent, reliable marker immediately beneath the Miocene interval, so we used it to define the base of the Miocene (Fig. 2). Downdip, across the Clemente-Tomas Fault Zone (e.g., McDonnell et al., 2009), the Anahuac is deep, occurring from depths of about 2100 m (7000 ft) to more than 3960 m (13,000 ft), is greatly expanded in thickness, and has been penetrated by few wellbores. In these downdip areas, most prominently in the upper (northeast) and far South Texas coastal offshore, we relied upon top of Oligocene contours published by Galloway (2001) to define the base of the Miocene.

Miocene Capacity Interval

Because of the greater volumetric efficiency of storing CO_2 in a supercritical or dense phase (Elewaut et al., 1996), the top of the Miocene capacity interval (CI) (Fig. 3) is defined as either the top of the Miocene section or 1006 m (3300 ft) depth, whichever is deeper. The 1006 m depth is the upper limit of the zone in which CO_2 is a supercritical fluid (Wallace et al., 2014). The base of the Miocene CI is defined as either the base of the Miocene stratigraphic section or the top of overpressure zone, whichever is shallower. Regional overpressure is typically encountered at depths of approximately 2438–3048 m (8000–10,000 ft) in the study area (Wallace et al., 1981; Pitman, 2011).

Although a detailed analysis of seals was beyond the scope of the project, Lu et al. (in press) have made a preliminary assessment of the trapping potential of Miocene mudrocks of the Texas offshore. Several regionally important seals occur in the Texas offshore Miocene, most prominently, the *Amphistegina* B (*Amph.* B) and the *Marginulina* A (*Marg.* A), but also included are the *Textularia* W and *Robulus* E/*Bigenerina* A mudrock zones (e.g., Figs. 2 and 3). There are also numerous, thinner mudrock units of more limited geographic extent with more localized trapping potential. In addition, many hydrocarbon traps have been found in OTSW Miocene reservoirs (e.g., Seni et al., 1997) demonstrating that the Miocene possesses mudrock units capable of trapping CO_2.

Capacity Calculations

Our OTSW regional static capacity estimate was performed using relatively dense empirical data sets for determining the fundamental parameters of reservoir thickness, average porosity and depth. In frontier areas where data are sparse, workers can employ the methods of spatial stochastic modeling, such as those demonstrated by Popova et al. (2014). Using the densely populated OTSW subsurface dataset, we generated parameters required for input to Equation 2. A Petra™ "Grid Model Calc Transform" was generated to calculate CO_2 capacity from the following input maps (grids):

(1) Depth to top of CI,
(2) Depth to base of CI,
(3) CI midpoint depth,
(4) CO_2 fluid density at CI midpoint depth,
(5) Net reservoir sandstone isopach of CI, and
(6) Average porosity of CI.

Structure and depth maps were made by interpreting stratigraphic boundaries from raster images (2900 wells) and LAS log suites (2142 wells). The stratigraphic boundary interpretations were guided by biostratigraphic reports (386 wells). The "Top of Geopressure" contours of Pitman (2011) were imported into our Petra™ database and were gridded and contoured. Net reservoir sandstone was determined from normalized spontaneous potential curve intervals defined by a cut-off value of -50 or less millivolts. Summations of the total footage of net reservoir sandstone that satisfied this condition were made for each well. Estimation of average porosity of the SP-defined net reservoir sandstone intervals was determined from sonic and density curves from 292 wells in the project area. CO_2 fluid density was determined from a Texas-Miocene specific transform developed by Nicholson (2012). The respective values for depth, CO_2 fluid density, net reservoir sandstone, and average porosity were gridded and contoured using Petra™. These input grids were used to calculate net regional capacity for the Miocene in the project area. Intermediate work products such as structure, isopach, isoporosity, and geopressure maps are not presented here, but can be found in Carr et al. (in press). Further workflow details can be found in Wallace et al. (2014) and Carr et al. (in press).

Capacity Results

Our recent static CO_2 net capacity estimate for the Miocene of the OTSW is 30.1 Gt of CO_2 (Fig. 4) (Carr et al., in press). We divided the Carr et al. (in press) OTSW capacity results into seven (7) sectors with similar CO_2 capacity potential (Fig. 4). Table 1 lists the net capacity results for the sectors. The average area of each sector is 1395 km^2 (539 mi^2), ranging from 815–1871 km^2 (315–722 mi^2), roughly comparable to the size of a Texas county (average 2664 km^2 [1029 mi^2]). On average, the capacity sectors contain 4.3 Gt CO_2 (14% of Total OTSW capacity), ranging from 1.2–8.0 Gt CO_2. There is not a strict correlation between sector area and sector CO_2 capacity because significant between-sector differences exist in CO_2 capacity per unit area, which averages 3.0 Mt/km^2 (7.8 Mt/mi^2) and ranges from 2.0–5.4 Mt/km^2 (5.1–14.1 Mt/mi^2).

There are significant uncertainties in the U.S. DOE regional static capacity calculations we have employed, including local variations in porosity, permeability, reservoir pressure, fluid saturations, internal heterogeneity, top seal characteristics, and faulting. These uncertainties are discussed at length in Goodman et al. (2011) and Wallace et al. (2014). For this high-level review of the static CO_2 capacity in the OTSW Miocene, the most important readily definable factors controlling capacity are the volume of net reservoir sandstone (or proxy "net-to-gross": the ratio of net reservoir sandstone within the gross stratigraphic interval), the depth of reservoir occurrence, and the depth of geopressure. The intent here is to provide broad guidance for reconnaissance resource estimation; it is not intended to be used at the prospect level. Further, in the words of Goodman et al. (2011), "As the site characterization process proceeds at individual CO_2 storage sites, additional site-specific data will likely be collected and analyzed, thereby reducing uncertainty."

Based on qualitative observations of sector capacity, its distribution within each sector, and source-sink relationships, we assigned informal labels that represent a qualitative ranking, ranging from "very favorable" to "unfavorable" (Table 1). We address each sector's CO_2 sequestration potential in the discussion below.

Capacity Sectors

Houston Sector: Very Favorable. A high net-to-gross ratio is present throughout the Miocene in the Houston sector. This is

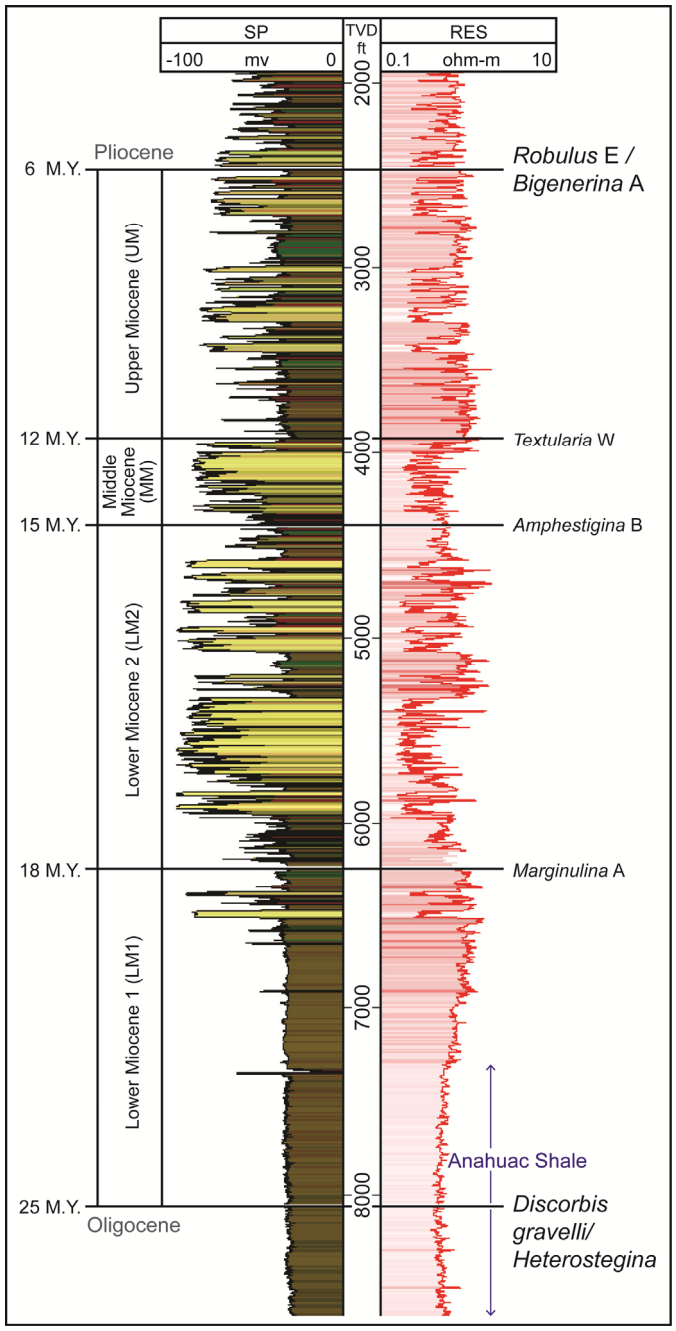

Figure 2. Type log of distal coastal and offshore Miocene interval showing major biostratigraphic tops (far right) used for regional interpretations, along with corresponding unit names (to left; Galloway et al., 2000), and geologic age (far left) (modified after Wallace et al., 2014). Wireline log curves: SP = spontaneous potential (black) and RES = deep resistivity (red).

readily visible in the strike-oriented cross section (Fig. 5A), where yellow highlighted areas of the spontaneous potential (SP) curves indicate the presence of porous and permeable reservoir sandstone bodies in the Middle Miocene (MM) and Lower Miocene, particularly in the Lower Miocene 2 (LM2) (Galloway et al., 2000). The LM2 is the Lagarto operational unit/Calcasieu delta system of Galloway (1989), which is dominantly comprised of delta-front and strandplain-shoreface sandstones found in traps set up by complex growth-fault and salt-related structures. Due to the overall eastward shift of the paleo–Red River depocenter (Galloway, 2001), deltaic facies are of lesser volume than strandplain-shoreface deposits in MM strata. Overpressure is deep (2438 m [8000 ft] to 3353 m [11,000 ft]) and thus, unlikely to interfere with sequestration objectives in the Houston sector.

The source-sink relationship here is not only excellent, but also fortuitous. The Houston sector contains the largest capacity of the OTSW, and this capacity occurs adjacent to the power plants, chemical plants, and refineries comprising the Houston metropolitan area's 131 point sources (EPA, 2015). These sources emitted 99 Mt of CO_2 equivalent (CO_2e) in 2014 (EPA, 2015), which is fully one-quarter of Texas' total CO_2 emissions (389 Mt CO_2e). The Houston sector's P_{50} CO_2 capacity estimate 8.0 Gt (or 8000 Mt CO_2e; Table 1) represents approximately 80 yr of CO_2 storage at 2014 EPA–reported emission rates.

Galveston Sector: Favorable. Although the Galveston sector is smaller than the Houston sector, its high net-to-gross ratio, particularly in MM and LM2 (Fig. 5B), good capacity per unit area (3.5 Mt/km^2; Table 1), and good source-sink match make it an attractive area for potential CO_2 sequestration. The sandstone reservoirs were predominantly deposited in the Matagorda barrier/strandplain system of Galloway (1989). The individual reservoirs are thicker and probably less heterogeneous than deltaic facies to the east, and thus can provide large quantities of pore space. However, the thickest, homogeneous MM sandstone bodies (up to 185 m [600 ft]) here generally lack sufficient structural closure and may also lack the seal integrity necessary to trap fluid columns equal to their thickness. Overpressure is relatively deep, but rises from approximately 2743 to 2438 m westward (9000–8000 ft) (Fig. 5B) and would increasingly interfere with sequestration objectives to the west.

A good source-sink match exists for the power and chemical plants and refineries in northeastern Galveston County, which emit 13 Mt CO_2e from a dozen point sources (EPA, 2015). This is particularly true in the northernmost part of the sector where good capacity per unit area is greatest (Fig. 5B).

Brazos Sector: Moderately Favorable. On the whole, the Brazos sector is poor on a capacity per unit area basis (2.0 Mt/km^2; Table 1), but CO_2 storage targets are present locally. Sequestration potential is moderate-to-good in the northern part because of source-sink matching with high net-to-gross intervals in the MM and LM2 unit, and also with moderate net-to-gross in the LM1 (Figs. 4 and 5C). As with the Galveston sector, the sandstone reservoirs were predominantly deposited in the Matagorda barrier/strandplain system (Galloway, 1989) although the sandstone volumes are comparatively lower here. Sequestration potential at the southern end is also good in the MM and LM2, but poor in the LM1 because of low net-to-gross and presence of overpressure, which rises above 2286 m (7500 ft) in some areas (Fig. 5C). Overpressure occurs at moderate depths of approximately 2134–2438 m (7000–8000 ft) (Fig. 5C), but rises higher locally where it may limit CO_2 storage in the LM1 and the lower parts of the LM2.

A good source-sink match exists for Brazoria County power plants, and chemical plants, and refineries, which emit 15 Mt CO_2e from 12 point sources (EPA, 2015), many of which are proximal to the northern extent of the sector, where capacity per unit area is greatest (Fig. 4).

Matagorda Sector: Favorable. The Miocene is structurally shallower in this sector than in the three easternmost sectors, and it thins southward reflecting the influence of the San Marcos Arch (Fowler, 1956; Halbouty, 1966; Galloway et al., 2000). Very high net-to-gross ratios in the LM2 and the LM1 of the southern portion (Fig. 5D) of the Matagorda sector result in moderately high capacity per unit area (3.3 Mt/km^2; Table 1). Overall CO_2 capacity is high at 4.9 Gt, which is second only to the Houston sector. The high net-to-gross may limit trapping locally in these Matagorda barrier/strandplain system (Galloway, 1989) deposits. The Upper Miocene (UM) unit has poor potential throughout due to occurrence above supercritical depth (1006 m

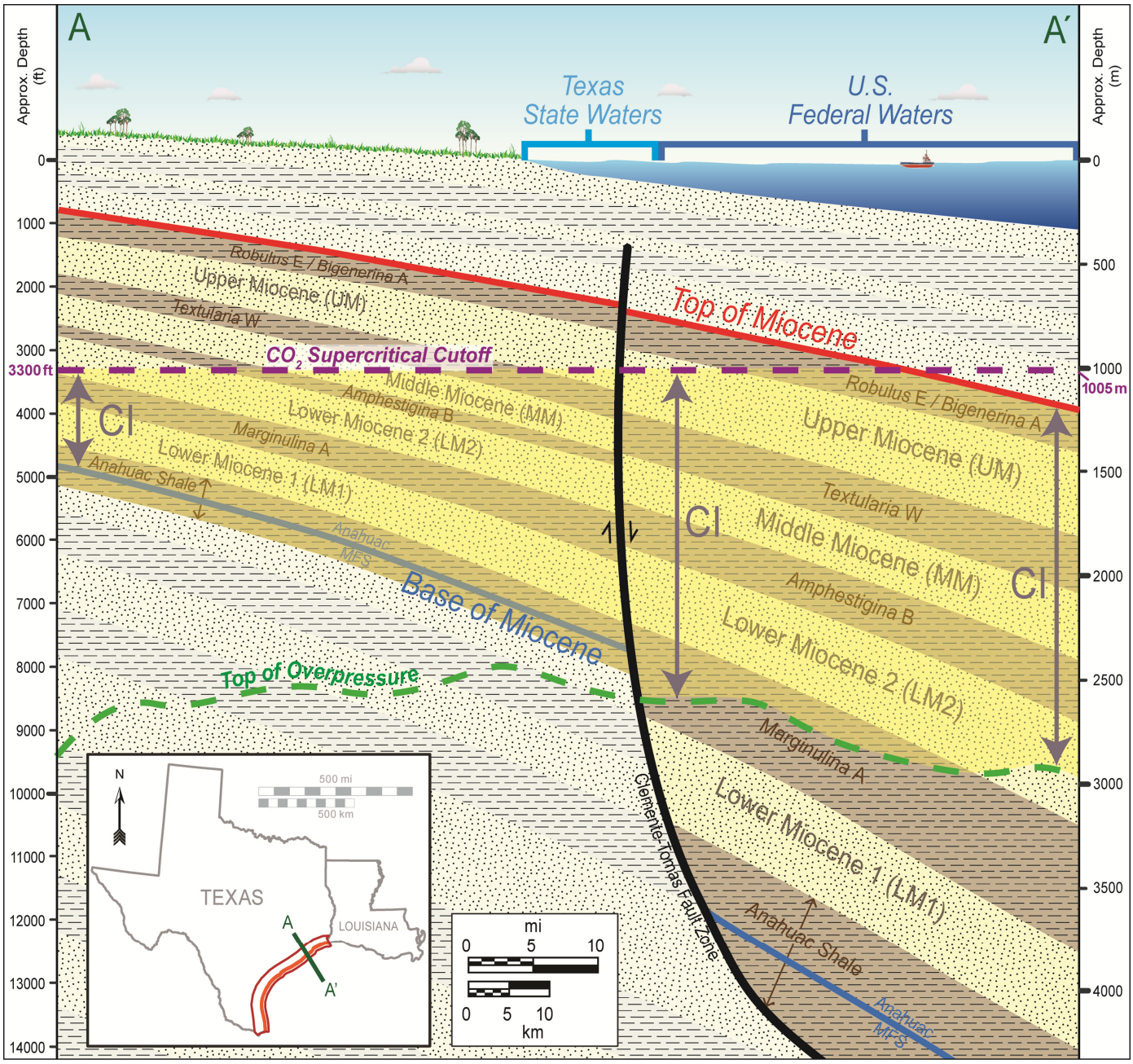

Figure 3. Schematic cross section showing the capacity interval (yellow) along with Miocene stratigraphy, with definitions from Galloway et al. (2000) (modified after Wallace et al., 2014). CI = capacity interval. The top of CI is defined as the top of either the Miocene or the CO_2 supercritical cutoff (1006 m [3300 ft]), whichever is deeper. The base of CI is defined as either the base of the Miocene or the top of overpressure, whichever is shallower.

[3300 ft]). The MM has similarly poor potential, except for on the seaward edge of northern portion of the sector, where the MM occurs below supercritical depth. The LM1 has moderate net-to-gross in the central and northern portions, but most of this thick section lies within overpressure.

There is a moderate source-sink match given that 6.6 Mt CO_2e from nine (9) point sources emanates from Calhoun (mainly) and Victoria County chemical plants and refineries (EPA, 2015).

Corpus Christi Sector: Moderately Favorable. Miocene strata are structurally shallowest and thinnest in this sector, where the influence of the San Marcos Arch (Halbouty, 1966; Galloway et al., 2000) is greatest. Almost all of the CO_2 sequestration potential in the Corpus Christi sector occurs in the Lower Miocene. The LM1 is the best target here due to high net-to-gross throughout the sector, and from northeast to southwest, the depositional environments grade from Oakville shoreline sandstones to North Padre deltaic sandstones (Galloway et al., 2000). There are also LM2 potential reservoirs in both the far northern and far southern portions of the Corpus Christi sector (Fig. 6A). The *Amph.* B shale lies at a depth of about 1070 m (3500 ft) here, which is essentially coincident with supercritical depth (1006 m [3300 ft]) (Figs. 3 and 6A). Thus, the UM and the MM have poor potential throughout the sector due to their occurrence above supercritical depth. Although depth to overpressure is relatively shallow (1829–2134 m [6000–7000 ft]) (Fig. 6A), it is roughly coincident with the top of the Anahuac Shale (Figs. 2 and 3) and thus, LM1 and the LM2 occur above overpressure in most of the sector.

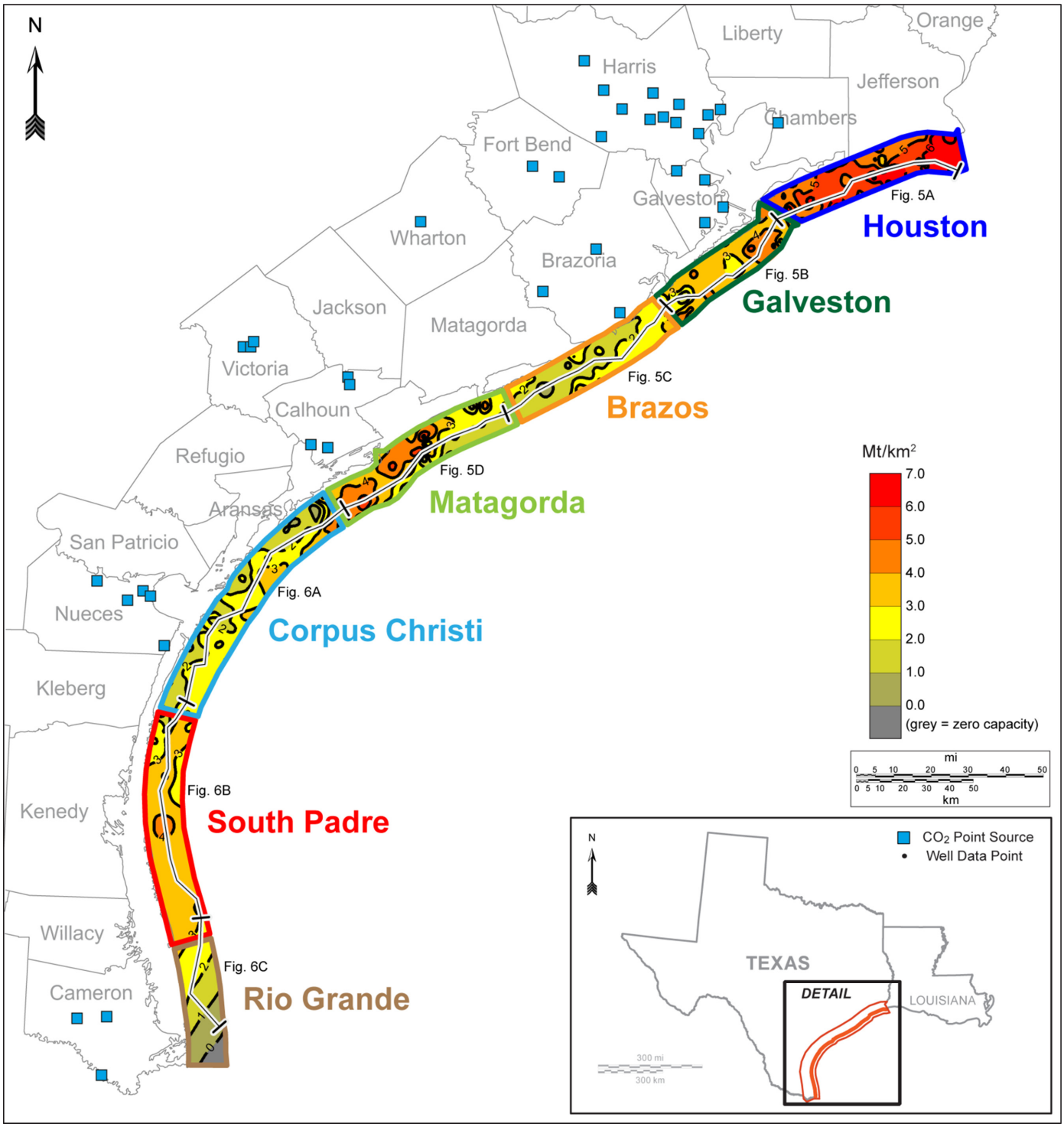

Figure 4. CO_2 isocapacity map (Mt/km^2) for offshore Texas State Waters (from Carr et al., in press). The map has been subdivided into 'capacity sectors.'

The total sector capacity of 4.1 Gt CO_2 is average and capacity per unit area is low (2.2 Mt/km^2; Table 1). However, capacity per unit area is low mainly because Corpus Christi is the largest sector in terms of area (1871 km^2 [722 mi^2]), which somewhat masks the fact that there are well-developed sandstone reservoir targets at relatively shallow depths (1524 m [5000 ft] to 2134 m [7000 ft]) throughout the LM1. Almost 5% of Texas' CO_2 emissions are located near the Corpus Christi sector, mostly in Nueces County (18.7 Mt CO_2e from 31 point sources; EPA, 2015), indicating that there is a reasonably good source-sink match here.

South Padre Sector: Favorable. Most of the sector's CO_2 sequestration opportunities occur in high net-to-gross North Padre delta sandstones of the LM2 and LM1 (Galloway et al., 2000). The influence of the San Marcos Arch (Halbouty, 1966; Galloway et al., 2000) is still evident in the northern portion of the sector, where net-to-gross is lower than it is in the downdip southern portion of the South Padre sector. The UM and the MM occur above supercritical depth (1006 m [3300 ft]) (Figs. 3 and 6B), except in southernmost portion where thin-bedded shelf to lower shoreface sandstones are present below supercritical depth.

Table 1. P_{50} CO_2 capacity estimates, offshore Texas State Waters (OTSW); Gt = 10^9 tonnes; Mt = 10^6 tonnes. Abbreviations for regional stratigraphic intervals of Galloway et al. (2000) (see Figure 2) are: UM = Upper Miocene, MM = Middle Miocene, LM2 = Lower Miocene 2, and LM1 = Lower Miocene 1. 2014 Annual CO_2 emissions from EPA (2015) from onshore areas adjacent to each sector.

Sector	Area, km^2 (mi^2)	CO_2 Capacity Estimate (P_{50}; Gt)	Average Capacity Per Unit Area, Mt/km^2 (Mt/mi^2)	% of TOTAL OTSW Capacity	2014 Annual CO_2 emissions, Mt CO_2e (# point sources)	Qualitative Sequestration Potential
Houston	1470 (567)	8.0 Gt	5.4 (14.1)	26.5%	99 Mt (131)	Very favorable
Galveston	1057 (408)	3.7 Gt	3.5 (9.1)	12.3%	13 Mt (12)	Favorable
Brazos	1385 (535)	2.7 Gt	2.0 (5.1)	9.0%	15 Mt (12)	Moderately favorable
Matagorda	1487 (574)	4.9 Gt	3.3 (8.6)	16.3%	6.6 Mt (9)	Favorable
Corpus Christi	1871 (722)	4.1 Gt	2.2 (5.7)	13.7%	18.7 Mt (31)	Moderately favorable
South Padre	1683 (650)	5.5 Gt	3.3 (8.5)	18.2%	0 Mt (0) [none reported]	Favorable
Rio Grande	815 (315)	1.2 Gt	1.5 (3.8)	4.0%	3.2 Mt (5)	Unfavorable
TOTAL Offshore Texas State Waters	9875 (3813)	30.1 Gt	3.0 (7.8)	100%	156 Mt (200)	na

Overpressure is deeper than 2750 m (9000 ft) in most of the South Padre sector (Fig. 6B) and would not be detrimental for CO_2 storage except in the LM1 to the far south.

The South Padre sector is centered on Kenedy County, one of the most sparsely populated counties in the nation (less than 1 person per mi^2; U.S. Census Bureau, 2010b). The EPA (2015) did not report any CO_2 emissions from either Kenedy or Willacy County. Despite the presence of good geological opportunities for CO_2 sequestration (5.5 Gt CO_2 capacity; 3.3 Mt/km^2; Table 1), there are no large point sources nearby.

Rio Grande Sector: Unfavorable. The best potential for CO_2 sequestration in the Rio Grande sector is in the thin-bedded distal deltaic and shore-zone sandstones of the UM (Galloway et al., 2000) (Fig. 6C), which have moderately good net-to-gross ratios that increase to the north. The LM1 and LM2 have very low net-to-gross. LM2 sandstone volume increases northward as distal shore zone and shelf sands transition to North Padre delta deposits (Galloway et al., 2000). The MM, LM2, and LM1 are precluded from sequestration by geopressure to the south, where the top to geopressure rises above 2134 m (7000 ft) (Fig. 6C). The LM1 has very little sequestration potential since it lies within geopressure in most of the Rio Grande sector, except locally in the northernmost portion, where there are distal North Padre delta sandstone reservoirs.

CO_2 emissions landward of the Rio Grande sector are mostly from Hidalgo County power plants (3.2 Mt CO_2e from 5 point sources; EPA, 2015). Better sequestration opportunities exist northward, either in the LM2 or the UM of the northern Rio Grande sector or in the LM2 and LM1 of the southern portion of the South Padre sector.

CONCLUSIONS

The purpose of this high-level resource assessment was to provide broad guidance for future, more detailed resource estimation and prospect development. Individual sequestration prospects will require specific understanding of technical details that are beyond the scope of this regional assessment. Some of these details are permeability, reservoir heterogeneity, reservoir pressure, fluid saturations, top seal characteristics, and faulting. In this regional assessment, the key factors controlling the static CO_2 capacity estimates were volume of net reservoir sandstone (or proxy net-to-gross ratio), reservoir depth (a pressure-fluid density proxy), and depth to regional geopressure.

Miocene strata of the offshore Texas State Waters (OTSW) hold an estimated potential resource of 30.1 Gt of CO_2 capacity (Carr et al., in press) (Fig. 4). The upper Texas coast sectors—Houston (8.0 Gt CO_2), Galveston (3.7 Gt CO_2) and Brazos (2.7 Gt CO_2)—together comprise almost half (47.8%) of the CO_2 capacity we estimated for the entire OTSW. The combined 2014 CO_2 emissions from landward facilities adjacent to the Houston, Galveston, and Brazos sectors represents 82% of Texas coastal emissions (Table 1). The Houston sector by itself, has excellent potential for geological CO_2 sequestration offshore from the Houston metro area's numerous power plants, chemical plants and refineries, which are responsible for 25% of Texas CO_2 emissions (EPA, 2015) (Table 1). The Houston sector's 8 Gt of estimated capacity represents about 80 yr of CO_2 storage at present emission rates.

The Corpus Christi sector is also important because point sources in the metro area release approximately 5% of Texas CO_2 (EPA, 2015). Although Miocene geological sequestration capacity is somewhat limited in this region due to stratal thinning over the San Marcos Arch and relatively shallow overpressure, there is still good sequestration potential in well-developed Lower Miocene sandstones. Although the Rio Grande sector has the poorest CO_2 sequestration potential for its 3.2 Mt emissions (less than 1% of Texas CO_2 emissions), there is available capacity to the north in the adjacent South Padre sector.

The OTSW's most important advantage is the excellent source-sink relationship between major coastal CO_2 point sources and the immediately adjacent—and large—volumes of potential offshore Miocene storage capacity. Other advantages of sequestering CO_2 in the Miocene of the OTSW are numerous, including simplified land rights (single owner, i.e., State of Texas), lack of groundwater issues, pre-existing infrastructure, deep geological and operational knowledge, and cultural familiarity with offshore subsurface operations. Clearly, the upper Texas coast should be a major focus of sequestration operations for Texas as well as the U.S. at large, given the sizable volume of CO_2 emissions there at present, coupled with the high potential for CO_2 sequestration in Miocene strata that we have identified.

ACKNOWLEDGMENTS

This research was supported by the National Energy Technology Laboratory (NETL) of the U.S. Department of Energy (DOE), and the Texas General Land Office (GLO). Neither

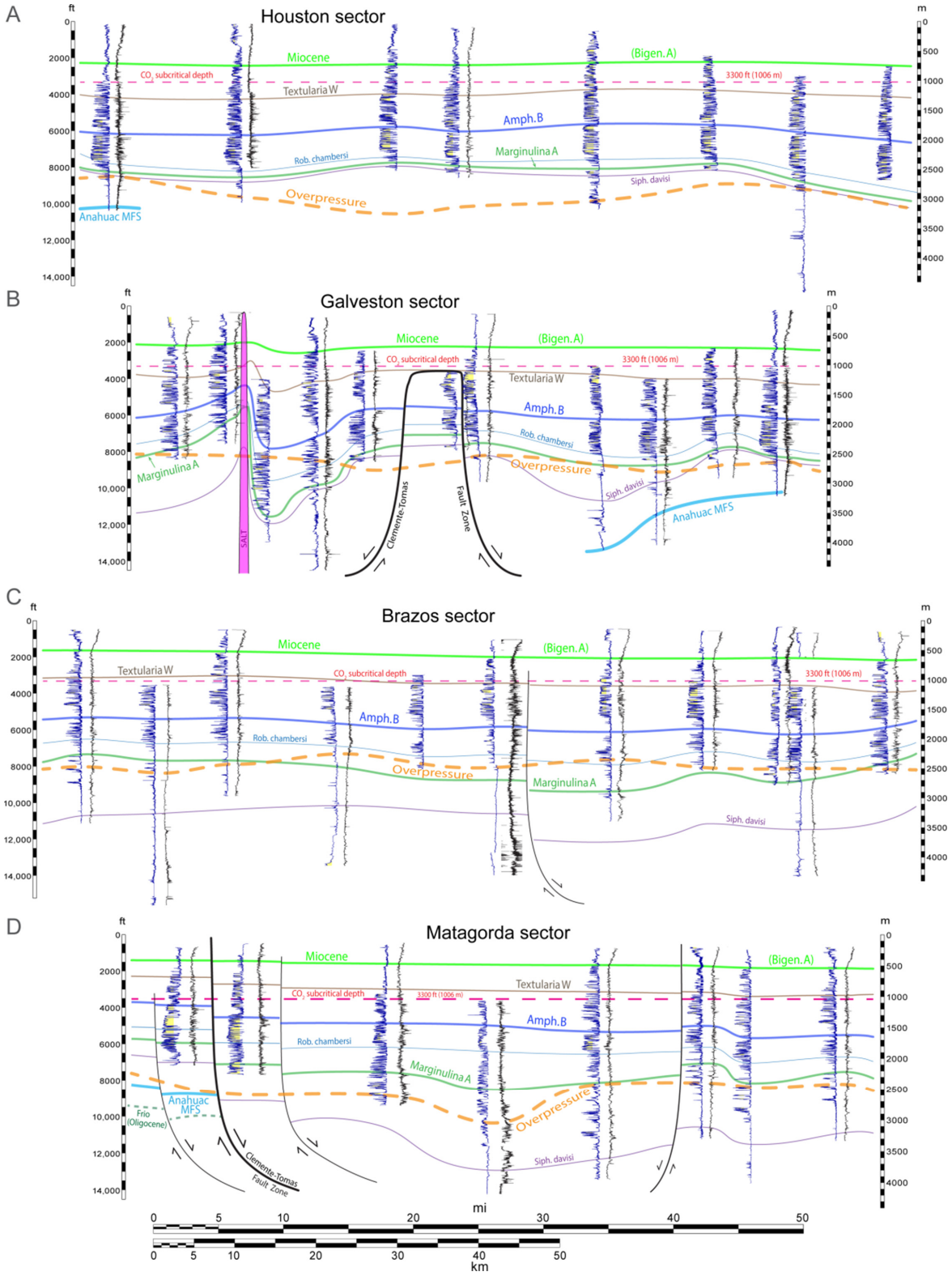

Figure 5. Strike-oriented, west-to-east cross sections through the offshore Texas State Waters capacity sectors: (A) Houston, (B) Galveston, (C) Brazos, and (D) Matagorda. Sector and cross-section locations are shown in Figure 4. Wireline log curves in the cross sections represent spontaneous potential (SP) in blue and resistivity in black. Shale volume from gamma-ray curves (VSH), represented in grey, shown for those wells where we lacked SP. Sonic delta t, represented in teal, was used in some cases where resistivity curves were not available. Yellow color-fill of the SP and/or VSH curves highlights net reservoir sandstone intervals, indicated by SP less than -50 mV or VSH less than 0.5 (Carr et al., in press). Stratigraphic unit boundaries are represented by various colored lines: Frio Fm. = dashed dark green; Anahuac maximum flooding surface (Anahuac MFS) = thick cyan; *Siphonina davisi* = purple; *Marginulina ascensionensis* = thick dark green; *Robulus chambersi*) = thin medium blue; *Amphistegina* B = thick blue; *Textularia* W = thick brown; top Miocene (*Bigenerina* A) = thick lime green; top CO_2 supercritical zone (-1006 m [-3300 ft]) = red dashed; top overpressure (Pitman, 2011) = orange dashed; and fault interpretations (schematic) = solid black lines. Vertical scales are relative to sea-level datum.

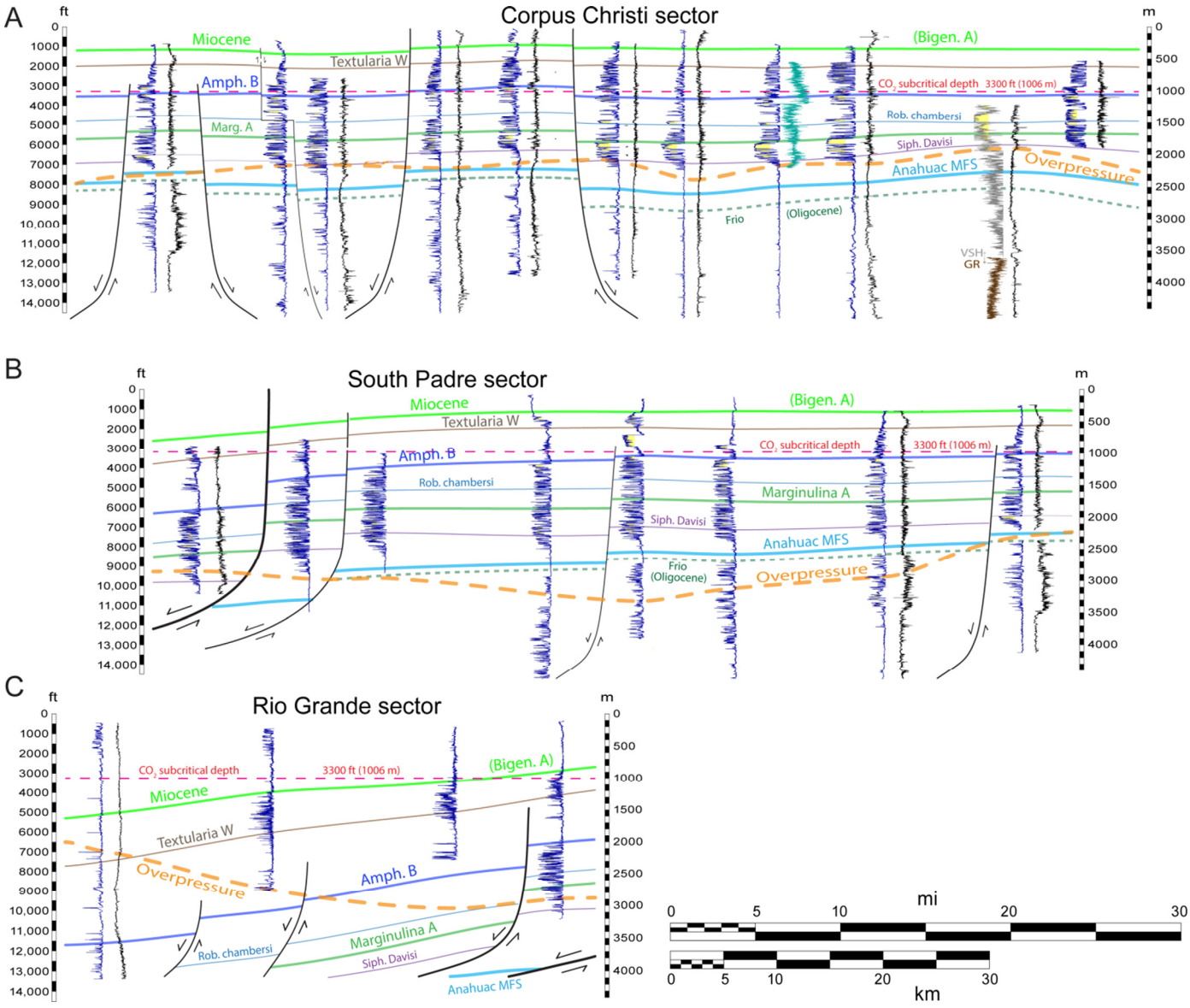

Figure 6. Strike-oriented, west-to-east cross sections through the offshore Texas State Waters capacity sectors: (A) Corpus Christi, (B) South Padre, and (C) Rio Grande. Sector and cross-section locations are shown in Figure 4. See Figure 5 caption for key.

the U.S. Government nor any agency thereof, nor any of their employees, makes any warranty, express or implied, or assumes any legal liability or responsibility for the accuracy, completeness, or usefulness of any information, apparatus, product, or process disclosed, or represents that its use would not infringe privately owned rights. Reference herein to any specific commercial product, process, or service by trade name, trademark, manufacturer, or otherwise does not necessarily constitute or imply its endorsement, recommendation, or favoring by the U.S. Government or any agency thereof. The views and opinions of authors expressed herein do not necessarily state or reflect those of the U.S. Government or any agency thereof.

The Bureau of Ocean Energy Management (BOEM; formerly Minerals Management Service) provided digital data (e.g., well information, directional surveys, biostratigraphic reports, and reservoir properties), free and available for download. Dr. William E. Galloway's deep knowledge of Gulf of Mexico sedimentology helped point us to the Miocene interval. Dr. Galloway's associates Patty Ganey-Curry and John Snedden of the Gulf Basin Depositional Synthesis group at the University of Texas Institute for Geophysics provided a considerable volume of contextual geologic information. Special thanks to William A. Ambrose, Kristen M. Carter, Ramón H. Treviño, and an anonymous reviewer for comments and suggestions that improved the manuscript.

REFERENCES CITED

Bachu, S., 2003, Screening and ranking of sedimentary basins for sequestration of CO_2 in geologic media in response to climate change: Environmental Geology, v. 44, p. 277–289.

Bachu, S., and W. D. Gunter, 2003, Acid gas injection in the Alberta Basin, Canada: A CO_2 storage experience: Geological Society of London Special Publications, v. 233, p. 225–234.

Bureau of Ocean Energy Management (BOEM; formerly Minerals Management Service), 2010, Paleontologic information, releasable paleo reports (downloaded ACSII data set files), <http://www.data.boem.gov/homepg/data_center/paleo/paleo.asp> Last Accessed April 17, 2013.

Carr, D. L., K. J. Wallace, A. J. Nicholson, and C. Yang, in press, Chapter 5: Regional CO_2 static capacity estimate, offshore

Miocene saline aquifers, Texas State Waters, *in* R. H. Trevino, ed., Geological CO_2 sequestration atlas for Miocene strata, Texas State Waters: Texas Bureau of Economic Geology Report of Investigations 282, Austin, Texas.

DOE (U.S. Department of Energy), 2015, Carbon storage atlas: National Energy Technology Laboratory, 5th ed., <http://www.netl.doe.gov/research/coal/carbon-storage/atlasv> Last Accessed August 11, 2016.

Eiken, O., P. Ringrose, C. Hermanrud, B. Nazarian, T. A. Torp, and L. Høier, 2011, Lessons learned from 14 years of CCS operations: Sleipner, In Salah, and Snøhvit: *Energy Procedia*, v. 4, p. 5541–5548.

Elewaut, E., R. van der Straaten, D. Koelewijn, H. E. Baily, S. Holloway, J. Barbier, E. Lindeberg, H. Moller, and K. H. Gaida, 1996, Inventory of the theoretical CO_2 storage capacity of the European Union and Norway, *in* S. Holloway, ed., The underground disposal of carbon dioxide: JOULE II Project CT92–0031 Final Report, British Geological Survey, Nottingham, p. 116–162 .

EPA (U.S. Environmental Protection Agency), 2015, Greenhouse gas emissions from large facilities; data was reported to EPA by facilities as of 8/16/2015, <http://ghgdata.epa.gov/ghgp/main.do> Accessed March 8, 2016.

Fillon, R. H., P. N. Lawless, and R. G. Lytton, III, 1997, Gulf of Mexico Cenozoic biostratigraphic and cycle charts: Gulf Coast Association of Geological Societies Transactions, v. 47, p. 271–282.

Fillon, R. H., and P. N. Lawless, 2000, Lower Miocene–early Pliocene deposystems in the Gulf of Mexico: Regional sequence relationships: Gulf Coast Association of Geological Societies Transactions, v. 50, p. 411–428.

Fowler, P., 1956, Faults and folds of south-central Texas: Gulf Coast Association of Geological Societies Transactions, v. 6, p. 37–42.

Gale, J., N. P. Christensen, A. Cutler, and T. A. Torp, 2001, Demonstrating the potential for geologic storage of CO_2: The Sleipner and GESTCO projects: Environmental Geosciences, v. 8, p. 160–165.

Galloway, W. E., 2001, Cenozoic evolution of sediment accumulation in deltaic and shore-zone depositional systems, northern Gulf of Mexico Basin: Marine and Petroleum Geology, v. 18, p. 1031–1040.

Galloway, W.E., 1989, Genetic stratigraphic sequences in basin analysis. I. Architecture and genesis of flooding-surface bounded depositional units: American Association of Petroleum Geologists Bulletin, v. 73, p. 125–142.

Galloway, W. E., P. Ganey-Curry, X. Li, and R. T. Buffler, 2000, Cenozoic depositional evolution of the Gulf of Mexico Basin: American Association of Petroleum Geologists Bulletin, v. 84, p. 1743–1774.

Goodman, A., A. Hakala, G. Bromhal, D. Deel, T. Rodosta, S. Frailey, M. Small, D. Allen, V. Romanov, J. Fazio, N. Huerta, D. McIntyre, B. Kutchko, and G.. Guthrie, 2011, U.S. DOE methodology for the development of geologic storage potential for carbon dioxide at the national and regional scale: International Journal of Greenhouse Gas Control, v. 5, p. 952–965.

Halbouty, M. T., 1966, Stratigraphic-trap possibilities in Upper Jurassic rocks, San Marcos Arch, Texas: American Association of Petroleum Geologists Bulletin, v. 50, p. 3-24.

Holloway, S., 2001, Storage of fossil fuel derived carbon dioxide beneath the surface of the earth: Annual Review of Energy and the Environment, v. 26, p. 145–166.

Lackner, K. S., 2003, A guide to CO_2 sequestration: Science, v. 300, p. 1677–1678.

Litynski, J. T., S. Plasynski, H. G. McIlvried, C. Mahoney, and R. R. Srivastava, 2008, The United States Department of Energy's regional carbon sequestration partnerships program validation phase: Environment International, v. 34, p. 127–138.

Lu, J., D. L. Carr, R. H. Trevino, J.-L. T. Rhatigan, and R. Fifariz, in press, Chapter 3: Evaluation of Lower Miocene confining units for CO_2 storage, offshore Texas State Waters, northern Gulf of Mexico, U.S.A., *in* R. H. Trevino, ed., Geological CO_2 sequestration atlas for Miocene strata, Texas State Waters: Texas Bureau of Economic Geology Report of Investigations 282, Austin, Texas.

McDonnell, A., M. R. Hudec, and M. P. A. Jackson, 2009, Distinguishing salt welds from shale detachments on the inner Texas shelf, western Gulf of Mexico: Basin Research, v. 21, p. 47–59.

Nicholson, A. J., 2012, Empirical analysis of fault seal capacity for CO_2 sequestration, lower Miocene, Texas Gulf Coast: Master's Thesis, University of Texas at Austin, 88 p., <http://repositories.lib.utexas.edu/handle/2152/ETD-UT-2012-05-5606> Last Accessed August 11, 2016.

Pitman, J. K., 2011, Reservoirs and petroleum systems of the Gulf Coast: Depth to top overpressure 2011 [map], <http://www.datapages.com/Services/GISUDRIL/OpenFiles/ReservoirsandPetroleumSystemsoftheGulfCoast.aspx> Accessed March 1, 2013.

Popova, O. H., M. J. Small, S. T. McCoy, A. C. Thomas, S. Rose, B. Karimi, K. Carter, and A. Goodman, 2014, Spatial stochastic modeling of sedimentary formations to assess CO_2 storage potential: Environmental Science and Technology, v. 48, p. 6247–6255.

Seni, S. J., T. F. Hentz, W. R. Kaiser, and E. G. Wermund, Jr., eds., 1997, Atlas of northern Gulf of Mexico gas and oil reservoirs: Volume 1. Miocene and older reservoirs: University of Texas at Austin, Bureau of Economic Geology, Gas Research Institute, Department of Energy, and Minerals Management Service, 199 p. plus plates and CD-ROM.

Tsang C. F., S. M. Benson, B. Kobelski, and R. E. Smith, 2002, Scientific considerations related to regulation development for CO_2 sequestration in brine formations: Environmental Geology, v. 42, p. 275–281.

U.S. Census Bureau, 2010a, State area measurements and internal point coordinates, <https://www.census.gov/geo/reference/state-area.html> Accessed September 5, 2014.

U.S. Census Bureau, 2010b, Census results—United States and Puerto Rico, population density by county or county equivalent, <http://www.census.gov/geo/maps-data/maps/thematic.html> Accessed March 9, 2016.

Vangkilde-Pedersen, T., K. L. Anthonsen, N. Smith, K. Kirk, F. Neele, B. van der Meer, Y. L. Gallo, et al., 2009, Assessing European capacity for geological storage of carbon dioxide—The EU GeoCapacity project: *Energy Procedia*, v. 1, p. 2663–2670.

Wallace, K. J., T. A. Meckel, D. L. Carr, R. H. Treviño, and C. Yang, 2014, Regional CO_2 sequestration capacity assessment for the coastal and offshore Texas Miocene interval: Greenhouse gases: Science and Technology, v. 4, p. 53–65.

Wallace, R. H., Jr., J. B. Wesselman, and T. F. Kraemer, 1981, Occurrence of geopressure in the northern Gulf of Mexico Basin: U.S. Geological Survey, 1 panel.